NIWA
Taihoro Nukurangi

Estimation of the target strength of oreo and associated species

Gavin Macaulay, Alan Hart, Paul Grimes, Roger Coombs, Richard Barr, and Adam Dunford

Final Research Report for
Ministry of Fisheries Research Project OEO2000/01A
Objective 1

National Institute of Water and Atmospheric Research

31 August 2002

Final Research Report

Report Title	Estimation of the target strength of oreo and associated species
Authors	Gavin Macaulay, Alan Hart, Paul Grimes, Roger Coombs, Richard Barr, and Adam Dunford

1. Date 31 August 2002

2. Contractor National Institute of Water and Atmospheric Research Limited

3. Project Title Estimation of the abundance of black and smooth oreo in selected areas

4. Project Code OEO2000/01A

5. Project Leader Gavin Macaulay

6. Duration of Project

Start date:	1 May 2000
Completion date:	31 August 2002

7. Executive Summary

Target strength to fish length relationships have been derived from swimbladder casts from 12 species of fish. These include smooth and black oreos, as well as the main oreo by-catch species.

In situ estimates of target strength for smooth and black oreos have been calculated from oreo marks observed during an acoustic survey and a Monte-Carlo method used to estimate swimbladder tilt distributions.

An anatomically detailed scattering model has been developed to that simulates the scattering of acoustic pulses from fish. Applications include estimating target strength, and acoustic species identification. In addition, computed tomography scans have been used to obtain estimates of the density and sound speed of smooth oreo tissue for use in future modelling studies.

8. Objectives

To estimate *in situ* target strength of black oreo, smooth oreo, and species associated with the two oreo species, including orange roughy.

9. Introduction

Black oreos (*Allocyttus niger*) and smooth oreos (*Psuedocyttus maculatus*) are widely distributed in the southern half of New Zealand's EEZ. They support a substantial fishery mainly on the southern slopes of the Chatham Rise. The management of any fishery requires some estimate of abundance and for oreos it has proved difficult to find an entirely satisfactory method for this. Acoustic methods, despite some difficulties, have proved to have the most potential for measuring absolute abundance of oreos. Acoustic estimation of absolute abundance using echo-integration (Burczynski 1979; Johannesson & Mitson 1983) requires some measure of the target strength of the various species involved. For oreos and the species associated with oreos, target strength remains an area of uncertainty.

Some initial acoustic target identification work was carried out on *Tangaroa* in October-November 1995 (McMillan & Hart 1995). During the 1996–97 fishing year, NIWA carried out further target identification work, made some initial estimates of target strength and collected preliminary survey data (MFish project DEOE04). This was followed by an initial survey of OEO 3A and 4 in November-December 1997 (*Tangaroa* voyage TAN9713, MFish project OEO9701). A further survey of OEO 4 was carried out in October 1998 (*Tangaroa* voyage TAN9812, MFish project OEO9801). Further mark identification and *in situ* data was collected in October-November 2000 and 2001 (*Tangaroa* voyages TAN0011 and TAN0117, MFish projects OEO2000/01A and OEO2000/01A). In addition, an acoustic survey of smooth oreo in OEO 4 was carried out in October-November 2001 (*Tangaroa* voyage TAN0117 and *Amaltal Explorer* voyage AEX0101, MFish project OEO2001/01).

This report presents target strength results derived from data collected during voyages TAN9713, TAN9812, TAN0011 and TAN0117. The results are presented in four parts:

1. Target strength estimates of oreo and by-catch species obtained from swimbladder casts.
2. *In situ* estimates of black and smooth oreo target strength.
3. Acoustic scattering simulations from orange roughy using an anatomically detailed scattering model.
4. Measurements of the density and estimates of the sound speed in oreos.

A paper describing the techniques used to obtain the *in situ* estimates has been submitted to the Journal of the Acoustical Society of America (Coombs & Barr submitted).

10. Methods

10.1 Collection of swimbladder casts

A physical representation of the swimbladder was obtained by injecting a dimensionally stable epoxy resin into the swimbladder of the freshly caught fish. Additives were used to optimise the working properties of the resin (Epiglass HT9000 resin and hardener with HT440 epispheres, HT330 microballoons, and HT110 extender glue). By varying the amount of additive, the physical properties of the unset mixture were altered to suit swimbladder size, swimbladder shape, and

strength of the swimbladder wall. For species where swimbladders were seldom undamaged a light dough-like mixture was used and this was pre-shaped to match the best injected examples then pressed into position within the swimbladder though a rupture point, or into the cavity that the swimbladder occupied.

The resin was injected into intact swimbladders using a syringe and needle. When required, two syringes were used – one to deliver the resin, and one to remove the gas at the same rate and time that the resin was being injected. The fish were laid on their dorsal surface and supported on either side during the injection and setting time. This ensures that the cast accurately represents the dorsal surface of the swimbladder. The resin was allowed to set and then removed from the fish and cleaned. Any obvious holes due to bubbles of gas were filled in with more resin.

Swimbladders can be quite elastic and the point at which they are full of resin is not always obvious when injecting them. To obtain consistent results, measurements of the buoyancy of each species were made by weighing the fish under water and in air. The difference between these two weights represents the lift required for neutral buoyancy. Fish encompassing the size range were measured in this way and a relationship between fish length and buoyancy derived and used to calculate the amount of resin to inject into each fish.

Black oreo swimbladders are particularly susceptible to bursting, with a low incidence of undamaged swimbladders. However there is a well defined swimbladder cavity on the dorsal surface of the body cavity. Due to the difficulty in establishing a realistic lift value for black oreos three different swimbladder volumes were used: 1%, 1.5% and 2% of body weight. Measurements were taken of intact swimbladders, from these it was established that the bladder occupied 80% of the available swimbladder cavity. Friable resin of each set volume, shaped to match the intact bladder shape, was pressed into the swimbladder cavity to give an imprint of the *in situ* dorsal bladder shape. The width of the swimbladder was confined by the cavity boundary and constrained by bladder length, shape and volume. As a comparison some casts were made that filled 100% of the cavity length.

Casts were only made from intact swimbladders that were not obviously over-inflated or badly distorted. Nevertheless, there was a substantial degree of subjectivity in deciding how full they should be, particularly the black oreo swimbladders which were of poorer quality.

10.1.1 Processing of swimbladder casts – method I

This processing technique was applied to fish samples collected during two *Tangaroa* voyages, one from 10 November to 19 December 1997 and the other from 28 September to 30 October 1998. Both voyages were on the South Chatham Rise.

The smooth oreo swimbladder casts, which were typically shaped like prolate spheroids (see upper panel of Figure 1), were cut into slices with a diamond saw along and at right angles to their long axis. The outlines were then digitized. The slices were 2.5 mm thick where the shape changed rapidly and 5 mm thick elsewhere. Black oreo casts, which had more the shape of a short sausage (see lower panel of Figure 1), were not sectioned. Instead representative measurements of diameter as a function of length

were made (A. Hart. private comm4unication). As the smooth oreo swimbladders were found to be largely circular in cross section it was decided to model both black and smooth oreo swimbladders as having cylindrical symmetry. This had the advantage of greatly reducing the complexity of the integrals needed to evaluate the swimbladders target strengths whilst providing a realistic physical model. This simplification was validated by comparing the target strength calculated from the actual swimbladder shapes and the cylindrically symmetric approximation, and was the difference was always less than 0.2 dB.

To assess the volume to which swimbladders were inflated for neutral buoyancy, fish were weighed in salt water, taking care that any trapped air bubbles were removed prior to weighing. A numerical technique for allowing for uncertainty in inflation level will be described in section 11.2.

Casts were made of 32 black oreo swimbladders covering a range of fish total length of 25.7-36.8 cm and 27 smooth oreos covering a length range of 22.0-54.0 cm.

The swimbladder measurements for both species were used to construct equivalent cylindrically symmetric spheroids. The scattering from these was then estimated using the Kirchhoff approximation (Clayton & Engquist 1977; McClatchie et al. 1996b). By using swimbladder models with cylindrical symmetry, the time for numerically evaluating the surface integral was reduced considerably compared to the fully general case.

10.1.2 Processing of swimbladder casts – method II

This processing technique was applied to swimbladder casts collected during two *Tangaroa* voyages, one from 22 October to 6 November 2000 and the other from 16 October to 14 November 2001. Both voyages were on the South Chatham Rise.

A selection of the casts collected were digitised using a 3D scanner and associated software (Polhemus 2000) to produce a set of connected triangles in 3D space that represents the surface of the swimbladder. Using the Kirchhoff-approximation model (Foote 1985; McClatchie et al. 1996b), the target strength at 38 kHz was calculated at angles of –40 to +40 degrees in steps of 1 degree. For every species except smooth and black oreo these data were convolved with a fish tilt-angle distribution with mean of 0 degrees and standard deviation of 15 degrees (after McClatchie et al., 1996), to obtain a tilt-averaged target strength estimate for each fish. The tilt-angle distributions for the oreos were obtained from the Monte-Carlo modelling presented in Section 11.2. As these were derived from *in situ* data on smooth and black oreo they were used in preference to the more generic figures in McClatchie et al.(1996b). The contribution from the fish body was not included, but is considered to contribute less than 5% of the total target strength (Foote 1980).

For all fish except for smooth and black oreo, the angle of the swimbladder relative to the dorsal surface of the fish was estimated from inspection of the fish, and when mounting the swimbladders for scanning they were oriented so that fish sagittal axis would have been horizontal. Any tilts were applied during the analysis.

For smooth and black oreos the tilt angle and standard deviation derived in the Monte-Carlo simulations was used (see Section 11.2). For smooth oreo the mean, rounded to zero decimal places, of the two estimates was used (tilt of 22° and standard deviation of 4°), and for black oreo a mean of 17° and a standard deviation of 8° were used. The offsets applied in the Monte-Carlo analysis were also applied to the swimbladder estimates; this was −1.1 dB for smooth oreo (the mean of the two smooth offsets) and −1.3 dB for black oreo.

10.2 Swimbladder attitude for smooth and black oreo

The swimbladder offset to the horizontal axis of the fish (a line joining the top of the mouth to the end of the vertebrae in the tail) was measured by filling the swimbladder with epoxy resin loaded with barium sulfate and taking x-ray photographs of the whole fish (see Figure 1). Five x-rays each of black and smooth oreos were taken and an initial estimate of the swimbladder tilt angle gave 27.3±2.6° for black and 20.6±0.9° for smooth oreos. As sample sizes were small these values should only be taken as a rough guide to swimbladder orientation. Nevertheless, they do show that the swimbladder offset in oreos is much greater than in more slender fishes such as Atlantic cod (Clay & Horne 1994) where values 5 and 9° were measured for larger cod, and 16-17° for smaller cod.

As we only consider the scattering produced by the fish swimbladders in this report when we derive swimbladder tilt angles by matching target strengths measured *in situ* with those modeled from swimbladders, our fits will give the tilt angle distribution of swimbladders in free swimming fish. This distribution is the combined effect of the body tilt distribution of the freely swimming fish together with the distribution of the swimbladder tilt relative to that of the fish body. We assume the tilt angle of free-swimming oreos in the wild to follow a normal distribution zero mean. With this assumption our measured swimbladder tilt angles can then be assumed to be tilts measured relative to the horizontal axis of the fish. However it must be remembered that the standard deviation of the derived swimbladder tilt distributions will contain a significant component of standard deviation from the tilt distribution of the free swimming fish.

10.3 In situ data

10.3.1 Data collection

A split beam version of NIWA's Computerised Research Echosounder Technology (*CREST*) (Coombs 1994) was used to collect the *in situ* target strength data. *CREST* is computer based, using the concept of a 'software echo sounder'. The transmitter was a switching type with a nominal power output of 80 W rms, an operating frequency of 38 kHz and a transmit pulse length of 0.32 ms (12 cycles). Time between transmits was 1.4 s. All four transducer quadrants (beams) were energised simultaneously from the transmitter but on receive the system operated as four semi-independent echosounders. Each receiver channel had dual broadband, wide dynamic range pre-amplifiers and dual serial analog-to-digital converters (ADCs) feeding a digital signal processor (DSP56002). Analog Devices AD7723 ADCs were used, operating in

'band-pass' mode at a conversion rate of 62.5 kHz (equivalent to a rate of 125 kHz in a conventional ADC). The ADC data were complex demodulated, filtered and decimated to 15.625 kHz. The filter was a 100 tap, linear-phase finite impulse response digital filter with a 3 dB bandwidth of 3.0 kHz. After filtering and decimation a 40 Log R time varied gain was applied and the results shifted to give 16 bit resolution in both the real and imaginary terms. These complex data were stored for later processing. The transducer used was a Simrad model ES38DD split-beam transducer with a depth rating of 1,500 m. The combined source level and transducer receive response (SL+SRT) was 48.8 dB re 1 V and the receiver gain at 1 m was 60.4 dB.

The split-beam transducer and receiver electronics were mounted in an open frame deployed on a 2 km tow cable. The frame was at depths of between 900 and 1,000 m. Data were collected whilst drifting or steaming at very slow speeds (<2 knots). The system was ordinarily used with a 38.1 mm diameter tungsten carbide calibration sphere suspended about 20 m below the transducer, allowing continuous *in situ* calibration of the acoustic system.

In addition to the acoustic equipment, the frame was fitted with a battery powered underwater camera and video recorder, with illumination provided by a bank of high intensity, green light emitting diodes. Camera data were recorded during most deployments.

10.3.2 Data processing

The *in situ* acoustic data were collected from *Tangaroa* during voyage TAN0011. Echosounder 'marks' that were expected to be either black or smooth oreos were located and the towed transducer deployed 50-100 m above the mark for 1-2 hours with the aim of maximizing the number of echoes captured from individual fish.

After collecting the acoustic data the marks were trawled to identify the fish and estimate their size composition. For the latter as many fish as possible were measured, where practical the whole catch. Fish were measured to the millimetre below using NIWA's electronic fish measuring system. We carried out 49 trawls and the main species caught were black and smooth oreos and orange roughy. The proportions of these species are shown in Figure 2. The numbers along the upper x-axis of the figure give the acoustic transect numbers associated with the trawls numbered on the lower x-axis.

The acoustic data were first filtered to remove echoes not originating from individual fish. Echoes were initially identified by locating peaks in the combined beam signal. The measurements from individual quadrants of the transducer were combined in pairs to calculate the position of the selected echoes in the beam (Ehrenberg 1979) and the amplitude corrected for the position in the beam. The maximum amplitude of each echo was then estimated by fitting a quadratic to the three values bracketing the peak of the echo. The maximum of this quadratic was taken as the target strength value for subsequent analysis. Selection of echoes from individual fish was based on the criteria given in Barr et al. (2000).

10.3.3 Data selection

We have been very selective in choosing the *in situ* target strength data for correlation with the target strength distributions derived from swimbladder modelling and fish length data and only data from acoustic transects which were made in regions where the associated trawl catches were strongly dominated by one or other oreo species were used. Smooth oreos formed more than 90 % of the trawl catches associated with transects d49, d50 and d52 (corresponding to trawls 35, 36, and 37) and for transects d32, d33 and d34 (trawls 24 through 30) more than 95 %. The *in situ* target strength distributions for transects d32 and d49 are shown in the lower and upper panels of Figure 3 respectively.

By using both the amplitude and phase data of our targets (see Barr et al., 2000) we have been able to identify the 4 modes in the target strength distribution shown in the lower panel of Figure 3. The sharp peak near –53.5 dB is thought to be produced by myctophids and the broader peak near –49 dB is possibly due to orange roughy, the latter peak being better characterized in the phase data (see Barr et al., 2001). The very broad mode near –67 dB we ascribe to bathypelagic zooplankton. A process of elimination leaves us with the peak near –44 dB being due to smooth oreos. In the data for transect d49, shown in the upper panel of Figure 3, only 3 peaks are evident. An enhanced peak near –67 dB, ascribed to bathypelagic zooplankton, a narrow peaks near –52 dB due to myctophids and a broader peak near -43.5 dB which we ascribe to smooth oreos.

We have added the grey shaded regions to Figure 3. These cover the range of target strengths that we consider to be specific to smooth oreo and to be largely uncontaminated by larger fish with air-filled swimbladders or by orange roughy. When fitting *in situ* target strengths to target strengths from swimbladder modelling, we evaluated the least squares fit in the Monte-Carlo simulation over this region. As such, our technique is an advance on directly ascribing a modal peak in target strength to modal peak in fish length yet it is more constrained than the general search technique suggested by Cordue *et al.* (2001).

From the trawls made in the same area as the acoustic transects, we obtained the smooth oreo length distributions presented in the lower panel of Figure 4. It can be seen that the trawls associated with transect d49 produced slightly larger fish than the trawls associated with transect d32. This length difference may explain why the peak smooth oreo target strength shown in the upper panel of Figure 3 is slightly stronger than the peak smooth oreo target strength shown in the lower panel of the same figure.

As can be seen from the trawl catch data in Figure 2 there were no trawl areas where the catch was >90 % black oreos. However trawls 46 and 49 were 73 % and 88 % black oreos respectively and the acoustic transects in the same area (d96 and d98) were therefore chosen to give *in situ* target strength data dominated by black oreos. The *in situ* target strength distribution for transect d96 is shown in Figure 5 and can be compared with the *in situ* data for the smooth oreo transect, d32, in the lower panel of Figure 3. Whereas there are very few smooth oreo targets stronger than –40 dB it can be seen that black oreo targets extend in range up to ~ –33 dB. The regions shaded light grey in Figure 3 and Figure 5 show the target strength range used for fitting smooth oreo targets. The dark grey region in Figure 5 covers the range of target strength data we assume to be dominated by black oreos and as for smooth oreos, only

these data were used in the Monte-Carlo simulation. The black oreo length distribution from trawls 42–49, is shown in the upper panel of Figure 4.

10.4 Monte-Carlo analysis of *in situ* and swimbladder data

Three experimental data sets were used in the Monte-Carlo modelling, swimbladder cast data, fish length distribution data and *in situ* target strength data. The latter were collected in the same area as that of the fish mark from which the fish length distribution was derived. The swimbladder measurements were combined with the length data and an assumed fish tilt-angle distribution to generate a target strength distribution. To do this a simulated population of fish with randomly chosen lengths matching the observed length distribution was created. Each fish was given a randomly chosen tilt angle such that the overall tilt angle distribution matched a chosen distribution. Each fish was also given a randomly chosen swimbladder, selected from the dataset of measured swimbladders, appropriately scaled for the fish length. The target strength of each fish was then estimated using the Kirchhoff procedure outlined in Section 10.1.1 above. To allow for the possibility of the swimbladder being under or over inflated (and other measurement errors), an additional scaling parameter was also used in the target strength calculations.

With this procedure, the tilt angle distribution and the inflation were the only elements for which we did not have direct experimental data. The tilt angle mean and standard deviation were varied and the sum of the squares of the deviations (least squares error) between computed and *in situ* target strength measurements estimated for each distribution. Both the mean tilt angle and the tilt angle standard deviation were varied from 0° to 30° in 1° steps giving 900 different fish distributions. Errors in estimating the correct bladder inflation or small errors in equipment calibration were accommodated, after the target strength distribution had been calculated, by scaling the whole distribution (i.e., applying an offset) in the range ±2 dB with a 0.1 dB resolution.

10.5 Anatomically detailed scattering model

A scattering model of fish has been developed that incorporates detailed data on the fish anatomy, and realistically models acoustic scattering from fish. The theoretical basis of the model is presented, followed by the numerical technique used to obtain solutions in the time domain. The methods used to obtain the fish property data are then discussed, followed by the details of the simulation runs.

10.5.1 Theoretical basis

The propagation of sound waves through a fish and surrounding water were modelled using the equations of motion for a lossless fluid with variable sound speed and density (Pierce 1989);

$$\frac{1}{c^2}\frac{\partial^2 p}{\partial t^2} = \nabla^2 p - \frac{\nabla p \cdot \nabla \rho}{\rho}, \qquad (1)$$

where c is sound speed, p acoustic pressure, t time, and ρ density. Sound speed, pressure and density vary with space, while the pressure also varies with time.

10.5.2 Solution of the equations of motion

A 3-dimensional finite-difference time-domain algorithm that was fourth-order in the spatial derivatives of pressure, second-order in the spatial derivatives of density and second-order in the time derivative of pressure was used to solve equation 1. The differencing equation used on the main part of the grid was as given by equation 1b in Aroyan et al. (2000), with the difference that the signs on the $P^m_{i+2,j,k}$, $P^m_{i,j+2,k}$, and $P^m_{i,j,k+2}$ terms in the density terms are negative instead of positive. Periodic boundary conditions were used on two of the dimensions (y and z), while a 3D version of the 2D absorbing boundary condition given by equation 12 of Tirkas (1992) was used in the x dimension. The grid points one in from the absorbing boundary were calculated using a second-order spatial derivative scheme.

A plane wave was introduced into the computational domain travelling in the $+x$ direction and the model time-stepped until the reflected pulse had formed. The computation domain was made sufficiently large so that scattered waves that travelled across the periodic boundary conditions did not interfere with the dorsal aspect reflected wave.

10.5.3 Density and sound speed from CT scans

Computed tomography scans were taken of four thawed orange roughy – details on each fish are given in Table 1. The scanner was a Siemens Somatom AR.C CT scanner. A scan was taken every 5 mm, with a slice thickness of 5 mm. Exposure was 3 seconds per slice, with a tube voltage of 130 kV and current of 70 mA. The field of view was 300 or 220 mm, depending on the scan, giving a transverse image resolution of 0.586 and 0.430 mm respectively (the 3rd dimension of the resolution volume is the slice thickness, 5 mm). A proprietary processing algorithm ("Body 4", a good general algorithm) was used to produce the CT images. The output from the scanner was a 16 bit unsigned integer for each resolution volume. Conversion from these data to physical density was achieved via

$$\rho = [(d - 1024) * 1.06] + 1006.2,$$

where ρ is the tissue density in kg/m^3 and d the value from the scanner (pers. comm., Neville Jopson). This relationship applies to the particular scanner and was derived from measurements of objects of known density, and is valid for $824 \le d \le 1324$, corresponding to densities of 794 to 1324 kg/m^3 and covers most soft tissue in the fish. Note that the subtraction of 1024 converts d into HU (Hounsfield) numbers, the standard form for CT scan values.

Sound speed was calculated using the density to sound speed relationship given in Aroyan (2001). Few detailed measurements of sound speed and density exist for orange roughy. Measurements of sound speed at a range of pressures and temperatures in lipid extracted from orange roughy (McClatchie & Ye 2000) gave a

value of 1470 m/s at 12°C and atmospheric pressure. This lies within the range of values obtained using Aroyan's relationship on orange roughy soft tissue. A more precise comparison of these results was not possible because the lipid was obtained from the entire fish and does not represent any identifiable part of an orange roughy. Phleger & Grigor (1990) measured the density of lipids in orange roughy and obtained a value of 903 kg/m^3 at 6°C, and found the source of the lipid (swimbladder, skin, bone, etc) made little difference to the density. This compares to the range of values obtained from the CT scans of 841-899 kg/m^3 at 12.5°C. The average of fish flesh density given by Shibata (1970) compares well to the average density obtained from the CT scans (1050 kg/m^3 compared to 1052 kg/m^3).

As in Aroyan (2001), all points with an HU value in the range 150-300 were given a constant sound speed of 1730 m/s, and all points above 300 were given a sound speed of 3450 m/s and taken to represent bone. In addition, all HU values less than –155 were taken to be air and the sound speed and density was set to that of seawater. This scheme attempts to account for the effect of density blurring in the transition from bone to soft tissue, and soft-tissue to air, and also re-immerses the fish in seawater.

The CT scan data from each fish were re-sampled using linear interpolation to give a grid spacing of 1.5 mm in each dimension. This is sufficient to model frequencies up to about 100 kHz, with at least 10 grid points per acoustic wavelength. For the simulations presented in this report the minimum number of grid points per wavelength were 12.4.

10.5.4 Simulations

The fish data were each placed in a computation region that was twice as wide and twice as long as the fish, and extended for approximately 500 mm above the fish – see Figure 6. The sound speed and density in this region were set to those of seawater with a salinity of 35.0 ppt, temperature of 6.0 °C and a depth of 1000 m (giving a density of 1032 kg/m^3 as calculated from the UNESCO equation of state given by Gill (1982) and sound speed of 1491 m/s, calculated from an algorithm given by Fofonoff & Millard, 1983).

Cosine modulated plane wave pulses with a frequency of 38 kHz and 0.32 ms in length were introduced into the region, travelling in the positive x-direction. The model was time-stepped until a reflected pulse had formed and travelled away from the fish. The pressure at a range of points in the domain was recorded, and subsequently demodulated using the quadrature amplitude option of the Matlab demod function (Mathworks 2001a). This gave the amplitude and phase of the reflected pulse as a function of time at a specific range from the fish. The target strength is then calculated as

$$TS = 20\log_{10}\left(\frac{pr}{p_i}\right),$$

where p is the peak of the demodulated pressure envelope pressure at range r and p_i the peak of the demodulated pressure envelope incident upon the fish.

11. Results

11.1 Swimbladder target strength estimates

A total of 346 swimbladders from 12 species were scanned and used to estimate target strength. A further 61 swimbladders reported upon previously (Macaulay et al. 2001b) were included in the analysis, giving a total of 407 swimbladders. The by-catch species were chosen with regard to their contribution to the uncertainty of the smooth and black oreo acoustic biomass estimates (pers. comm., Ian Doonan) and the ease of obtaining swimbladder casts. As target strength estimates became available during the course of this project, the species that we thought contributed the most uncertainty changed – the species presented here include all fish from which we obtained swimbladders, and were obtained from trawls in and around smooth and black oreo marks.

The data fall within the range of points for gas filled swimbladder fish as given in Figure 3 of McClatchie et al. (1996a), indicating that the results are not atypical. The coefficients for regressions of the form $< TS >= m \log_{10}(L) + c$ (where $<TS>$ is the tilt-averaged target strength in dB re 1 m^2, m is the slope, L the fish length in cm, and c the intercept) are given in Table 2, and were calculated using the Matlab (Mathworks 2001b) robustfit function, an implementation of an iteratively re-weighted least-squares regression (Holland & Welsch 1977). The standard deviation of the distribution of the vertical distance of the actual points from the regression line is also given. The regressions and the associated target strength data are presented in Figure 7 for each species individually, while Figure 8 contains all the regressions, allowing comparison of target strength between species. All regressions are drawn over the size range of the fish used for the swimbladder casts.

The number of casts obtained for each species varied considerably. More effort was put into the smooth and black oreo, but we attempted to obtain 30 scans for each species. The goodness of fit of the regressions is particularly good for some species, for example ridge scaled rattail, but less so for other species such as serrulate rattail where the smaller fish have a much higher target strength than would have been expected from extrapolating the data for the larger specimens.

The swimbladder injection technique is not guaranteed to produce casts that are exact replicas of the swimbladder of the fish *in-situ*. This is mainly due to the depth at which the fish are found – the journey to the surface in a trawl net is not kind to the fish (they are usually dead or moribund and have lost most of their scales), and swimbladders are frequently burst or distended by the time the fish arrives at the surface.

Most of the backscattered energy comes from the dorsal surface of the swimbladder (Barr 2001) and this is the most important part of the swimbladder for modelling (assuming that fish spend most of their time 'upright'). This applies to geometrical scattering only and will not be applicable to Rayleigh scattering or resonance of the swimbladder (for which the swimbladder volume is more important). We have found that the shape and size of the dorsal surface of the swimbladder is constrained by the vertebrae of the fish and is captured well by the resin in spite of damaged swimbladders. This is particularly so for fish which have a pronounced wave-like

structure on the dorsal surface due to the vertebrae. As a result, the target strengths calculated from the swimbladder casts are considered to be representative of the target strength of the actual fish. However, for black and smooth oreo it proved difficult to eliminate all small bubbles of trapped gas – a number of fish from which an intact gas filled swimbladder had been removed were positively buoyant despite all efforts. Consequently for oreos it is assumed available lift values are biased low. The maximum lift value measured for smooth oreo was 1.2% of body weight, with a mean of 0.5%. For black oreo the maximum measured lift value was 0.8%, however this species has more areas that could harbour trapped gas. The larger swimbladder in black oreos, and larger in situ target strength indicates black oreo lift values are likely to be greater than smooth oreos of the same length.

Smooth oreo bladders are less prone to bursting due to a presumed venting of gases into the abdominal cavity, releasing pressure in the bladder as the fish ascends in the net. Intact swimbladders were injected with resin in situ resting in the swimbladder cavity with a target volume of 1% body weight. In practise swimbladders were found to be full at volumes less than 1%, and the mean volume injected was measured to be 0.7% of the body weight.

As discussed earlier, the swimbladders in black oreos were very fragile and injecting the swimbladder with resin was not practicable – imprints were taken instead. Varying the amount of resin used for the imprint casts resulted in small changes in target strength. These data are given in Figure 9. The difference in the target strength to fish length regression between casts with 1% and 2% swimbladder volume ranged from a maximum of 0.9 dB at 25 cm to a minimum of 0 dB at approximately 37 cm. Allowing the cast to occupy the entire swimbladder cavity produced a maximum difference at fish length 25 cm of 0.6 dB when compared to a 1% volume cast at 80% of the swimbladder cavity length. The minimum difference was 0.3 dB at 40 cm. Differences between casts at 1.5% and 1% of fish weight were of a similar magnitude as for the 2% and 1% casts. It is not clear which, if any is more correct – but see section 11.3 for further discussion on this. There is a general trend of increasing target strength with larger swimbladders, but the maximum difference is always less than 1 dB.

Several swimbladder scanned surfaces were saved with different triangle sizes to determine sensitivity target strength to commonly used surface resolutions. The resulting target strengths were within 0.02 dB of each other.

The repeatability of the scanning process was tested by scanning the same cast multiple times and re-calculating the TS each time. In all cases the target strengths were within 2% of each other.

11.2 Monte-Carlo analysis of *in-situ* data

In all the results presented in this section, the agreement between *in situ* target strength distributions and those computed from swimbladder models is shown as a 'goodness of fit.' This is evaluated as the reciprocal of the square root of the sum of the squares of the differences between measured and computed target strength. The fit is only evaluated over a limited range of target strengths. The regions shaded light and dark gray in Figure 5 show the target strength range limits for fitting smooth and

black oreo data respectively. The lower and upper panels in Figure 10 show the goodness of fit surfaces evaluated for the *in situ* data files d32 and d49. These surfaces, in mean tilt angle/tilt angle standard deviation space, were each evaluated using a swimbladder scaling offset. The scaling adjustments required the target strength, evaluated from the swimbladders, to be reduced by 1.6 dB to best fit data from file d32 and 0.6dB to best fit data from file d49.

The results from the two *in situ* target strength datasets are very similar in that they both show the presence of a single clear peak in the goodness of fit. Both datasets are also best fitted by very similar swimbladder orientation parameters, mean tilt angles of 20.8° and 22.4° and tilt angle standard deviations of 3.9° and 3.7° for files d32 and d49 respectively. The data in Figure 11 show the good agreement between *in situ* and modeled target strength distributions using these parameters.

Figure 12 shows the goodness of fit surface evaluated for the black oreo *in situ* data, file d96. The figure is plotted with a scaling adjustment of −1.3 dB, which was required to give the best overall goodness of fit. Again there is a clear region of enhanced goodness of fit. In this case the region is centered on a mean tilt angle of 17° with a standard deviation for the optimum tilt distribution of 8°. The minor peaks in goodness of fit, either side of the major peak, are thought to result from the statistical noise at the peak of the black oreo *in situ* target strength distribution (see Figure 5).

Figure 13 shows the computed target strength distribution based on this tilt angle distribution compared with the *in situ* measurements. The two plots can be seen to be in excellent agreement, especially when one remembers that the curves are only constrained to fit in the region shaded gray. The excellent fit over the target strength range from −30 to −50 dB suggests that there were few smooth oreos present in the region surveyed. From the mean tilt angle and tilt angle standard deviation values required to best fit the *in situ* target strength data, it is possible, using a Monte-Carlo simulation, to derive the target strength versus length distributions describing smooth and black oreos. These distributions are presented in Figure 14, the small circles representing the results of the Monte-Carlo simulation. The two lower curves, for smooth oreo data, can be seen to be very similar to each other and are displaced about 5 dB below the plot for black oreos. This 5 dB displacement appears to be almost independent of fish length, for fish of the length typically caught in the oreo fishing grounds around New Zealand.

The solid lines in Figure 14 are simple functional fits to the simulated points which can be used, for example, in biomass estimation. For black oreos the target strength, *TS*, of a fish of length, *L*, is given by:

$$TS = -78.05 + 25.3\log_{10}(L) + 1.62\sin(0.0815L + 0.238) \qquad (2)$$

For smooth oreo data files d032 and d049 the functions are of the form,

$$TS = -83.78 + 25.5\log_{10}(L) + 1.068\sin(0.111L - 1.59) \qquad (3)$$ and

$$TS = -80.54 + 23.76\log_{10}(L) + 0.987\sin(0.122L - 1.94) \qquad (4)$$ respectively.

These formulations were chosen by inspection of the residuals which resulted when fitting the data to simple logarithmic plots. They are not based on any insight into the physics of the scattering process. They do however provide extremely good fits to the computations.

In fitting the *in situ* target strength data using the theoretical target strength data computed from swimbladder casts we have made a number of assumptions. We have neglected changes in air density in the swimbladder with depth, we have neglected the scattering effects of the body of the fish and to allow for over or under inflation of the swimbladder we have applied a variable scaling shift to the theoretical target strength values to obtain an overall best fit between theory and experiment.

All theoretical estimates of target strength computed from our swimbladder database have had to be reduced to best fit the *in situ* data, on average by about 1.1 dB. This suggests either a possible offset in the computer models, over-inflation of swimbladders during casting or *in situ* target strength calibration errors. As the *in situ* data were calibrated in real time, using a calibration sphere suspended below the transducer, we think this latter suggestion the least likely. One weakness of our simple computer models was the lack of allowance for air density increase in the swimbladder which would serve to reduce the density contrast with the fish body and hence reflectivity. A simple calculation based on theory in Medwin and Clay (1998) indicates this approximation resulted in an overestimate of target strength by ~0.45 dB for fish at depths of 1,000 m. This reduces the difference between the *in situ* data and modeling to only 0.7 dB to be accounted for by fish body effects and/or swimbladder over-inflation. This appears to be excellent agreement between theory and experiment. The mean fish tilt angles of smooth oreos of 20.8° and 22.4°, determined from fits to the *in situ* data, are also in excellent agreement with the value of 20.6±0.9° determined from measurements on fish radiographs. The mean tilt angle of 17°, derived from modeling black oreo *in situ* target strength data, is not nearly such a good fit to the value of 27.3±2.6° derived from the black oreo radiographs. More work is needed in this area and possible causes of the difference are:-

- Distortions in the fish body or swimbladder. Most black oreo swimbladders burst on being brought to the surface.

- Contamination of the black oreo *in situ* target strength data by a significant presence of smooth oreos.

- Non zero mean tilt response of swimming black oreos. It must be remembered that the mean tilt angles measured in our modelling are the sum of the mean tilt angle of the swimbladder in the fish plus the mean tilt angle of the fish body when the fish is swimming through the water.

- Unduly small swimbladder tilt angles could result from using a model with too small a scaling offset, caused in turn by under-inflation of the swimbladders.

Changing the amplitude scaling factor is not a completely independent operation to changing the swimbladder tilt when it comes to evaluating a change in the target strength. To show this effect we have fixed the smooth oreo swimbladder tilt angle standard deviation at 4° and then allowed mean tilt angle and scaling factor to vary

together to best fit the *in situ* data for file d49. Figure 15 (lower panel) shows how the goodness of fit maximizes when the scaling correction is -0.6 dB. However the goodness of fit changes only slowly with scaling correction. Also plotted in the same figure is the mean tilt angle as a function of the scaling offset required to keep the goodness of fit maximized. It can be seen that the scaling offset and tilt angle are almost equivalent in their effect with a 1 dB scaling change being equivalent to a 2.9° change in mean tilt angle. Since Macaulay et al. (2001a) estimate target strength uncertainties due to incorrect swimbladder inflation to be a maximum of about 1 dB this translates to an uncertainty of 2.9° in our mean swimbladder orientation estimates. Figure 15 (upper panel) shows a similar plot for the black oreo data file d96. It can now be seen that the goodness of fit shows a clear peak at a scaling offset of −1.3 dB and a tilt angle of 17°. However, were the scaling offset to be >0 dB then a tilt angle of >20° would be more appropriate and more in line with the x-ray data.

Although the interdependence of scaling offset and tilt angle is annoying when one is trying to make deductions about fish biology and fish behaviour, it is of only minor importance when we consider biomass estimation. What is important for biomass estimation is that we have produced a mathematical fish model which accurately describes the *in situ* target strength data.

Having derived tilt angle distributions and scaling factors appropriate for free swimming black and smooth oreos we are now in the position to be able to apply the Monte-Carlo modelling technique to finding the proportions of black and smooth oreos solely from *in situ* acoustic data. This is discussed further in Coombs & Barr (submitted).

11.3 Comparison of swimbladder and Monte-Carlo *in situ* target strength

The length to target strength relationships presented in Section 11.2 are included in Figure 8 to allow comparison with those derived from the more recent swimbladder work presented in Section 11.1.

These results indicate that the cylindrically symmetric swimbladder Kirchhoff method (Section 10.1.1) for black and smooth oreo gives similar results to those from the full 3D-scanned swimbladder Kirchhoff results (Section 10.1.2).

Smooth oreo were injected with resin *in situ* resting in the swimbladder cavity with a target volume of 1% body weight. In practise swimbladders were found to be full at volumes less than 1% – the mean volume injected was measured at 0.7% of body weight. If we accept that the smooth oreo swimbladders were under inflated, this would explain, to some degree, the 1-2 dB difference between the Monte-Carlo results and the swimbladder results evident in Figure 8.

If one is willing to move away from a linear <TS> to fish length relationship, the curves give a better fit to the swimbladder data, and as shown in the Monte-Carlo section, agree well with the *in situ* data. The shape of the length to target strength curve is likely to be different for each species and will depend on the shape of the swimbladder and how it changes as the fish increases in length. Without any information to the contrary we recommend using the curve fits for smooth and black

oreo, but to remain with the linear length to target strength relationship for other species.

11.4 Orange roughy model target strength

The anatomically detailed scattering model of orange roughy is still under development, and is not producing credible target strength results. The scattering field results, however, are credible, and an example is presented in Figure 16 and Figure 17 where the wave field scattering by an orange roughy is given. The retardation of the acoustic wave by the swimbladder (with a lower sound speed than the rest of the fish) can be clearly seen in Figure 16. Note also the complicated scattered field in Figure 17.

Further development and checking of the model is required. This will be carried out as part of Objective 3 of MFish project ORH2001/01 in which the model will be used to develop techniques for acoustically identifying species groups in and around low density orange roughy marks.

12. Oreo tissue density and sound speed

Using the relationships presented in section 10.5.3, estimates of the density and sound speed in smooth oreo has been calculated, and are presented in Table 3. There was insufficient resolution in the CT data to confidently separate bone from surrounding tissue, however there is a well-defined peak at approximately 195 HU in the spine data and it is probably safe to assume that this is a hard tissue value rather than bone. The spread for bone (essentially a subset of the 'spine' data) is probably due to volume blurring and it may be more useful to specify a range (250-400) and use the median value. There are insufficient points to accurately determine the HU value for the otoliths, however in the absence of any other data this is probably a reasonable estimate of the lower bound – again due to volume blurring with the less dense surrounding tissue. The density of the eye was surprisingly high, and appears to be due to dense tissue in the lens. Density values and sound speed values were not calculated for the spine and bone due to uncertainties with volume blurring. This is also the reason for not giving sound speed values for the eye and otoliths.

13. Use of underwater camera in association with acoustic equipment

Camera data were recorded for most deployments. However, visibility was usually poor and the range limited. Salps were commonly seen but only one clear fish image was recorded (a shark of indeterminate species) and it was not seen acoustically at the same time.

An alternative approach, which could make use of equipment already available, is to use a single shot digital camera with flash illumination. This device has been used with considerable success on recent seamount surveys and it could be modified, without too much difficulty, to be triggered only when the echosounder system recorded a target within visible range, and for which a valid target strength value had been obtained. This would mean the limited capacity of the recording system would be used to maximum advantage. In fact with some processing, at a later stage, it may

be possible to just illuminate targets just within a known range of acceptable target strengths and echo characteristics.

Target identification is one of the main sources of uncertainty in oreo by-catch *in situ* data (this includes orange roughy) and a technique for improving the identification of acoustic targets is very desirable. For this reason, further work using underwater cameras is considered desirable.

14. Conclusions

Target strength/fish length relationships have been derived from casts of swimbladders from basketwork eels, black javelinfish, black oreo, notable rattail, serrulate rattail, four rayed rattail, robust cardinalfish, deepsea cardinalfish, Johnson's cod, ridge scaled rattail, smooth oreo, and white rattail. The swimbladder estimates presented in this report are the first to be produced for many of these species, and as such should be treated as initial estimates. Greater confidence in these results would be achieved by collecting *in situ* target strength data from these species in their natural environment, in a similar manner to smooth and black oreo.

Simple acoustic backscatter models of fish, based on measurements of swimbladder casts have been used to compute target strength distributions of black and smooth oreos for direct comparison with target strength distributions measured *in situ*. Only 3 parameters were used in the computer model: mean tilt angle, tilt angle standard deviation and an amplitude scaling factor. The latter was necessary to allow for uncertainties in swimbladder inflation during the manufacture of swimbladder casts. We found the following:

- Contours of goodness of fit between theoretical and experimental target strength distributions show single isolated maxima.
- The values of mean swimbladder tilt angle derived from this fitting process are in good agreement with swimbladder tilt angles measured from x-rays, particularly for smooth oreos.
- The agreement between measured and computed target strength distributions is excellent.
- There may be some uncertainties in the derivation of biological data on fish (tilt angle distributions versus swimbladder inflation) using our acoustic modelling technique, especially for black oreos. However we believe the target strength—length relationships we have derived by Monte-Carlo modelling are a significant step forward over the more basic technique of matching modes in the target strength and length distributions.

An anatomically detailed scattering model has been developed to that simulates the scattering of acoustic pulses from fish. Applications include estimating target strength, and acoustic species identification.

Measurements of the tissue density and sound speed in smooth oreo have been taken, and will be of use for future models of oreo target strength.

15. Publications

Coombs, R.F.; Barr, R. (submitted). Acoustic remote sensing of swimbladder orientation and species mix in the oreo population on the Chatham Rise. *Journal of the Acoustical Society of America.*

16. Data Storage

Data collected from trawling is stored in the Ministry of Fisheries Trawl survey database. Acoustic data is stored in the Ministry of Fisheries Acoustic database.

17. References

Aroyan, J.L. (2001). Three-dimensional modeling of hearing in *Delphinus delphis*. *Journal of the Acoustical Society of America 110(6)*: 3305-3318.

Aroyan, J.L.; McDonald, M.A.; Webb, S.C.; Hildebrand, J.A.; Clark, D.; Laitman, J.T.; Reidenberg, J.S. (2000). Acoustic Models of Sound Production and Propagation. *In*: Au, W.W.L.; Popper, A.N.; Fay, R.R. (eds). Hearing by Whales and Dolphins, pp. 485, Springer-Verlag, New York.

Barr, R. (2001). A design study of an acoustic system suitable for differentiating between orange roughy and other New Zealand deep–water species. *Journal of the Acoustical Society of America 109(1)*: 164-178.

Barr, R.; Coombs, R.F.; Dunford, A. (2001). *In situ* target strength measurements and chirp responses of orange roughy (*Hoplostethus atlanticus*). Final Research Report to the New Zealand Ministry of Fisheries. 45 p.

Barr, R.; Coombs, R.F.; Macaulay, G. (2000). "Can we discriminate between different deepwater fishes using a standard acoustics target strength ping?" *In*:Bradley, S. (ed) Presented at the Proceedings of the 10th International Symposium on Acoustic Remote Sensing of the Atmosphere and Oceans and Associated Techniques, Auckland, New Zealand, November/December 2000.

Burczynski, J. (1979). Introduction to the use of sonar systems for estimating fish biomass. Fisheries Technical Paper. 89 p.

Clay, C.S.; Horne, J.K. (1994). Acoustic models of fish: The Atlantic cod (*Gadus Morhua*). *Journal of the Acoustical Society of America 96(3)*: 1661–1668.

Clayton, R.; Engquist, B. (1977). Absorbing Boundary Conditions for Acoustic and Elastic Wave Equations. *Bulletin of the Seismological Society of America 67(6)*: 1529-1540.

Coombs, R.F.; Barr, R. (submitted). Acoustic remote sensing of swimbladder orientation and species mix in the oreo population on the Chatham Rise. *Journal of the Acoustical Society of America.*

Cordue, P.L.; Coombs, R.F.; Macaulay, G.J. (2001). A least squares method of estimating length to target strength relationships from *in situ* target strength distributions and length frequencies. *Journal of the Acoustical Society of America 109(1)*: 155-163.

Ehrenberg, J.E. (1979). A comparative analysis of *in situ* methods for directly measuring the acoustic target strength of individual fish. *IEEE Journal of Oceanic Engineering OE–4(4)*: 141-152.

Fofonoff, P.; Millard, R.C., Jr (1983). Algorithms for computation of fundamental properties of seawater. UNESCO Technical Papers in Marine Science. 53 p.

Foote, K.G. (1980). Importance of the swimbladder in acoustics scattering by fish: A comparison of gadoid and mackerel target strengths. *Journal of the Acoustical Society of America 67(7)*: 2084–2089.

Foote, K.G. (1985). Rather–high–frequency sound scattering of swimbladdered fish. *Journal of the Acoustical Society of America 78(2)*: 688–376.

Gill, A.E. (1982). Atmosphere-Ocean Dynamics. Academic Press Limited, 622 p.

Holland, P.W.; Welsch, R.E. (1977). Robust regression using iteratively reweighted least-squares. *Communications in Statistics: Theory and Methods A6*: 813-827.

Johannesson, K.A.; Mitson, R.B. (1983). Fisheries acoustics: A practical manual for aquatic biomass estimation. FAO Fisheries Technical Paper (240). 249 p.

Macaulay, G.J.; Hart, A.; Grimes, P. (2001a). Estimation of the target strength of orange roughy by-catch species. Research Progress Report to the Ministry of Fisheries. 10 p.

Macaulay, G.J.; Hart, A.; Grimes, P. (2001b). Estimation of the target strength of orange roughy by-catch species. Final Research Report to the Ministry of Fisheries. 11 p.

Mathworks. (2001a). Signal Processing ToolBox User's Guide. The Mathworks, Inc., Natick, MA. 560 p.

Mathworks. (2001b). Statistics ToolBox User's Guide. The Mathworks, Inc., Natick, MA. 560 p.

McClatchie, S.; Aslop, J.; Coombs, R.F. (1996a). A re–evaluation of relationships between fish size, acoustic frequency, and target strength. *ICES Journal of Marine Science 53*: 780–791.

McClatchie, S.; Aslop, J.; Ye, Z.; Coombs, R.F. (1996b). Consequence of swimbladder model choice and fish orientation to target strength of three New Zealand fish species. *ICES Journal of Marine Science 53*: 847–862.

McClatchie, S.; Ye, Z. (2000). Target strength of an oily deep–water fish, orange roughy (*Hoplostethus atlanticus*) II. Modeling. *Journal of the Acoustical Society of America 107(3)*: 1280–1285.

McMillan, P.J.; Hart, A.C. (1995). Voyage report for the 1995 south Chatham Rise oreo surveys (TAN9511). Unpublished report held in NIWA library, Wellington. 11 p.

Medwin, H.; Clay, C.S. (1998). Fundamentals of acoustical oceanography. *Applications of modern acoustics.* Academic Press, Boston. 712 p.

Pankhurst, N.W.; McMillan, P.J.; Tracey, D.M. (1987). Seasonal reproductive cycles in three commercially exploited fishes from the slope water off New Zealand. *Journal of Fish Biology 30*: 193-211.

Paul, L.J. (1986). New Zealand Fishes: An Identification Guide. Reed Methuen, Auckland. 184 p.

Phleger, C.F.; Grigor, M.R. (1990). Role of wax esters in determining buoyancy in *Hosplostethus atlanticus* (Beryciformes: Trachichthyidae). *Marine Biology 105*: 229–233.

Pierce, A.D. (1989). Acousitcs: An Introduction to Its Physical Principles and Applications. 2nd. Acoustical Society of America, Woodbury, New York, 678 p.

Polhemus (2000). User Manual for the FastSCAN hand held laser scanner. 47 p.

Shibata, K. (1970). Study on Details of Ultrasonic Reflection from Individual Fish. *Bulletin of the Faculty of Fisheries of Nagasaki University 29*: 1-82.

Tirkas, P.A.; Balanis, C.A.; Renaut, R.A. (1992). Higher order absorbing boundary conditions for the finite-difference time-domain method. *IEEE Transactions on Antennas & Propagation 40(10)*: 1215-1222.

18. Acknowledgements

The authors wish to thank the officers and crew of *Tangaroa* for their efforts in supporting the sea-going part of this project.

Table 1: *Details on the four orange roughy that were CT scanned. The staging method is described in Pankhurst et al. (1987).*

Fish	Length (cm)	Sex	Stage	Weight (g)	Scanned in	Voxel size (mm)
1	38.0	Female	4	1 746	Air	0.586, 0.586, 5.0
2	36.2	Female	4	1 846	Water	0.430, 0.430, 5.0
3	30.1	Male	3 or 4	818	Water	0.430, 0.430, 5.0
4	33.3	Female	2 or 6	1 321	Water	0.430, 0.430, 5.0

Table 2: Target strength/fish length relationships for oreo and oreo by-catch species (<TS> = *slope* * log10 (*fish length*) * *intercept*, where <TS> has units of dB re 1 m^2 and fish length has units of cm.). The fit is defined at the standard deviation of the distribution of the vertical distance of the actual points from the regression line.

Species code	Name	Intercept(dB)	Slope (dB/cm)	Fit	n	Av. Lift (%)
BEE	Basketwork eel (*Diastobranchus capensis*)	-70.1	20.1	1.2	30	2.4
BJA	Black javelinfish (*Mesobius antipodum*)	-84.5	25.9	1.2	16	1.0
BOE(a)	Black oreo (*Allocyttus niger*)	-62.4	14.9	1.0	27	1.0
BOE(b)		-64.9	16.9	1.0	29	1.5
BOE(c)		-56.9	11.7	1.2	14	2.0
BOE(d)		-62.1	14.9	1.6	30	1.0
CAS	Oblique Banded Rattail (*Caelorinchus aspercephalus*)	-80.4	28.0	0.9	30	
CIN	Notable rattail (*Coelorinchus innotabilis*)	-93.9	35.8	0.7	15	3.2
CSE	Serrulate rattail (*Coryphaenoides serrulatus*)	-93.8	34.6	1.7	20	3.2
CSU	Four rayed rattail (*Coryphaenoides subserrulatus*)	-84.6	26.3	1.4	32	3.2
EPR	Robust cardinalfish (*Epigonus robustus*)	-83.6	34.4	1.4	36	3.7
EPT	Deepsea cardinalfish (*Epigonus telescopus*)	-86.6	34.6	1.1	8	
HJO	Johnson's cod (*Halargyreus johnsonii*)	-70.3	22.5	0.8	28	3.0
MCA	Ridge scaled rattail (*Macrourus carinatus*)	-80.8	27.9	0.8	53	2.8
SSO	Smooth oreo (*Pseudocyttus maculates*)	-87.7	27.6	1.8	44	0.5
WHX	White rattail (*Trachyrincus aphyodes*)	-80.2	28.8	1.2	25	3.1

*BOE (a) volume 1% of fish weight, length 80% of abdominal cavity, BOE (b) volume 1.5% of fish weight, length 80% of abdominal cavity, BOE (c) volume 2% of fish weight, length 80% of abdominal cavity, BOE (d) volume 1% of fish weight, length 100% of abdominal cavity.

Table 3: Density and sound speed values calculated from a CT scan of an adult smooth oreo.

Tissue type	Mean HU value	ρ (kg/m^3)	c (m/s)	
Flesh	39	1 048	1 605	
Eye	214	1 233	-	
Spine	216	-	-	
Bone	296	-	-	
Otolith	850-900	1 907	-	

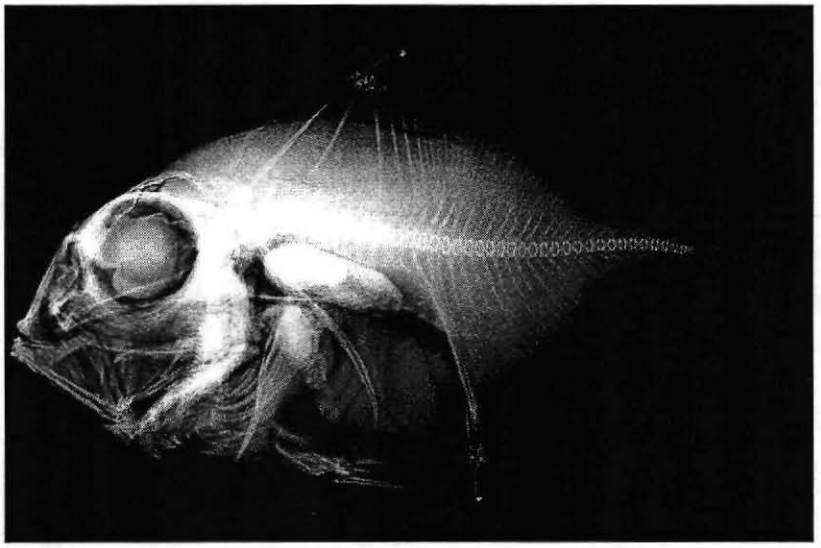

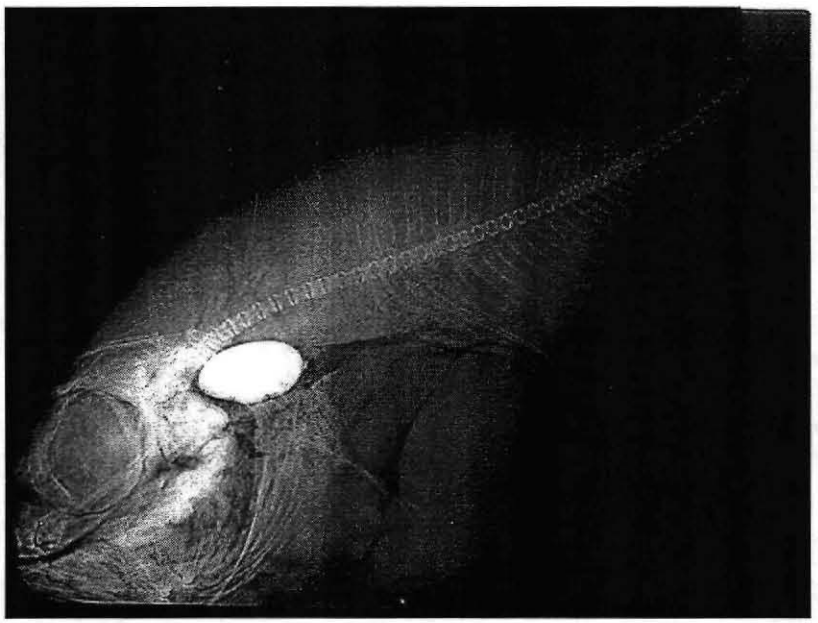

Figure 1: Lower panel: X-ray of a smooth oreo with a 'barium loaded' swimbladder. Upper panel: X-ray of a black oreo with a 'barium loaded' swimbladder.

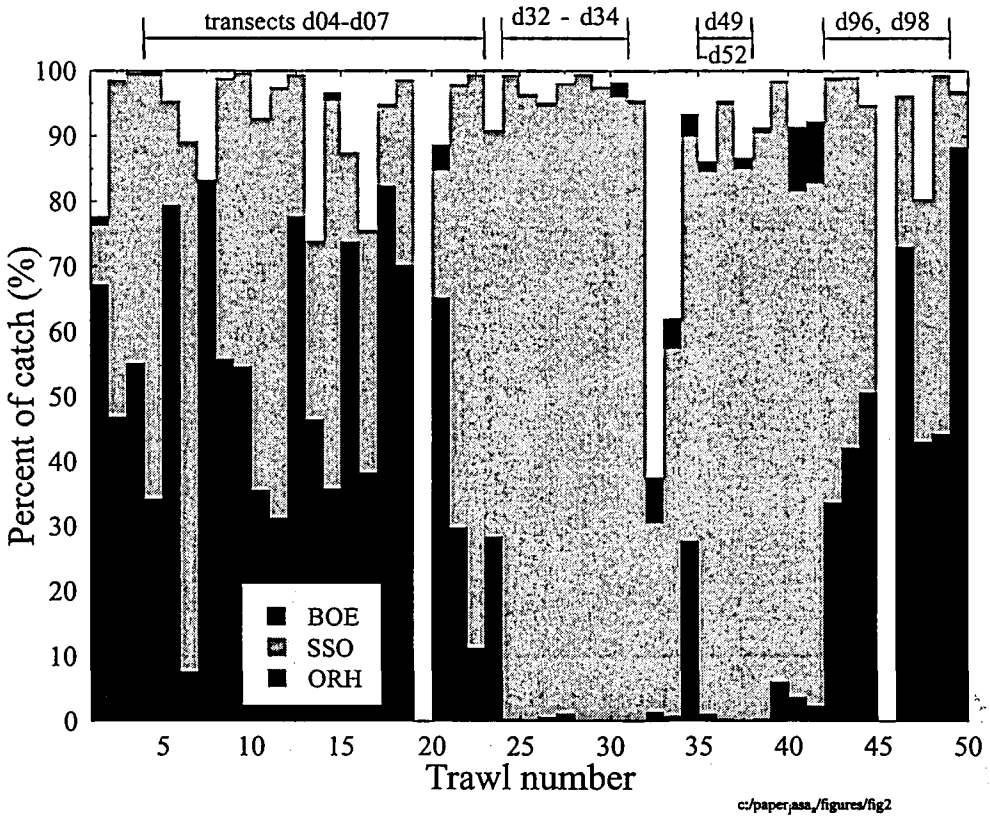

Figure 2. Percentage of black oreo (BOE), smooth oreo (SSO) and orange roughy (ORH) in trawl catches.

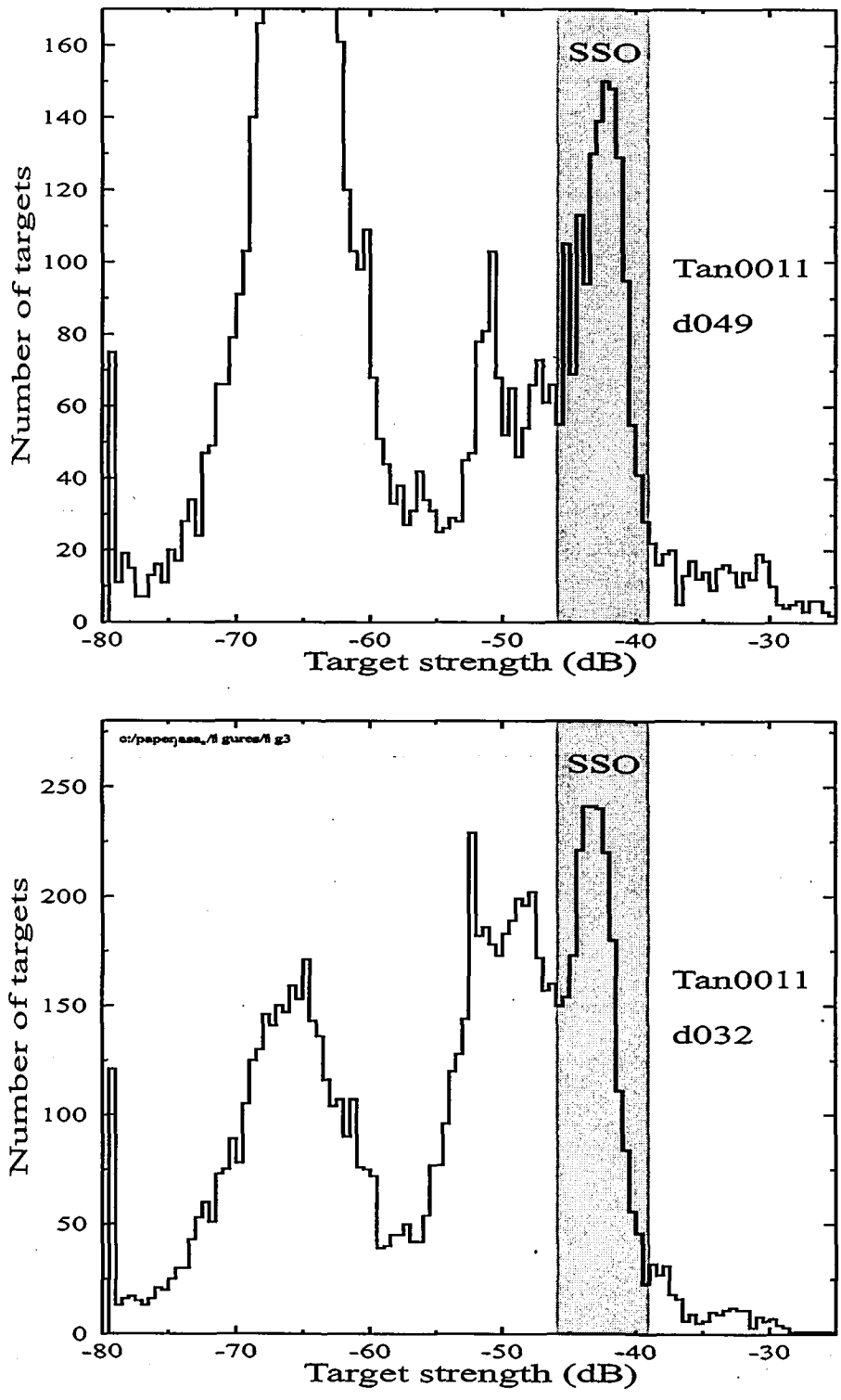

Figure 3. ***In situ*** **target strength distributions. Lower panel: transect d32. Upper panel: transect d49.**

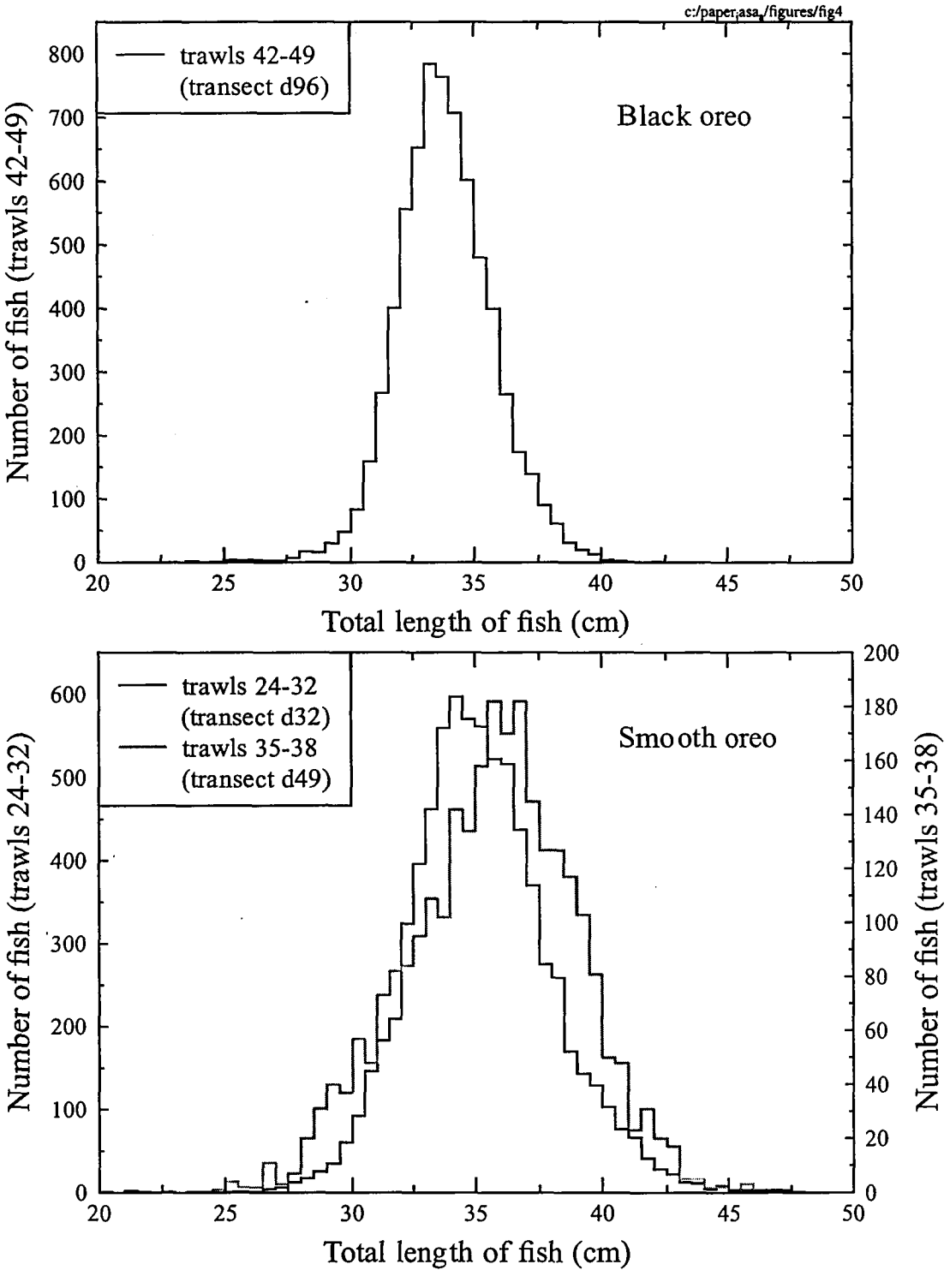

Figure 4. Fish length data. Lower panel: Trawl data associated with smooth oreo acoustic transects d32 and d49. Upper panel: Trawl data associated with black oreo acoustic transect d96.

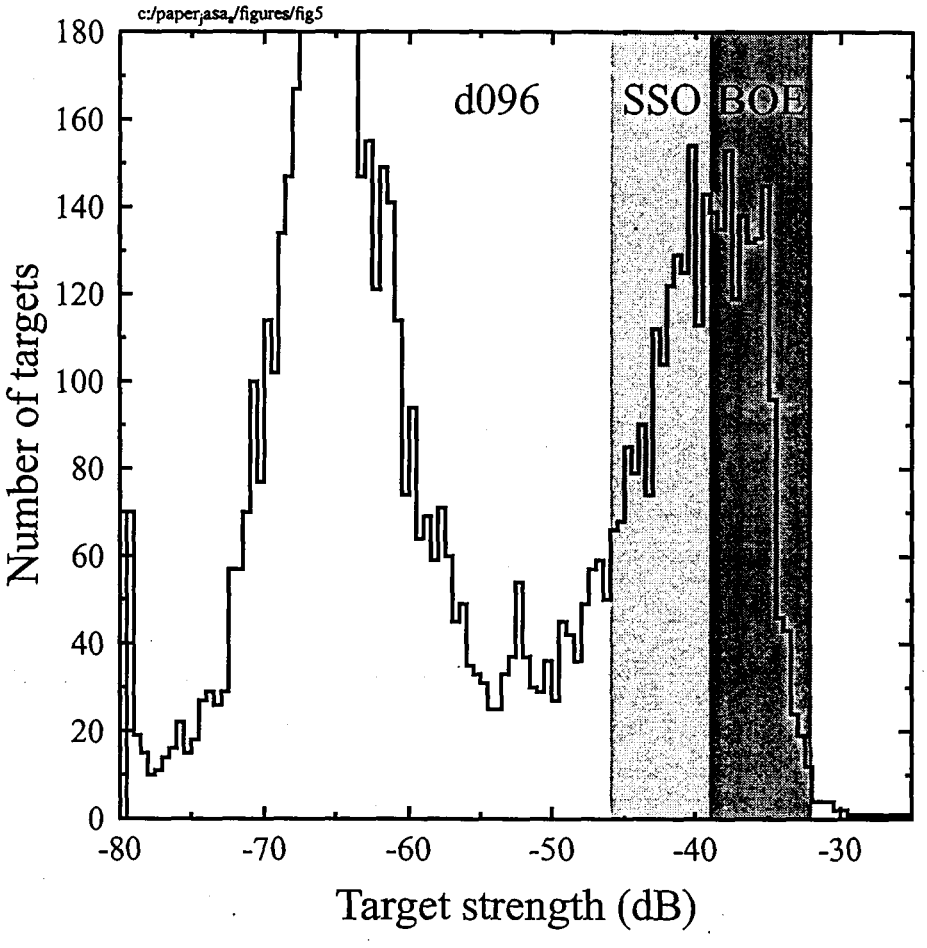

Figure 5. ***In situ*** **target strength data for transect d96.**

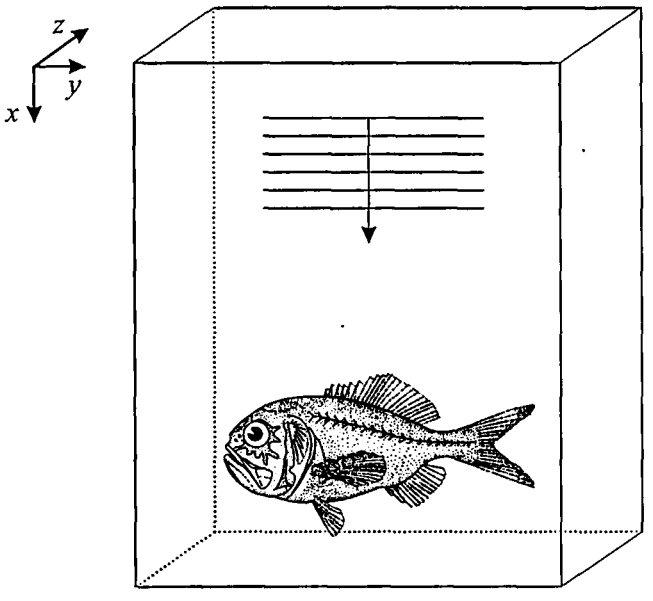

Figure 6. The simulation geometry indicating the location of the fish. The arrow indicates the direction of travel of the incident wave. The two boundary surfaces perpendicular to the *x*-axis absorb incident waves, while the other four are periodic. The dimensions of the volume varied to suit the size of the fish. The orange roughy drawing is from Paul (1986).

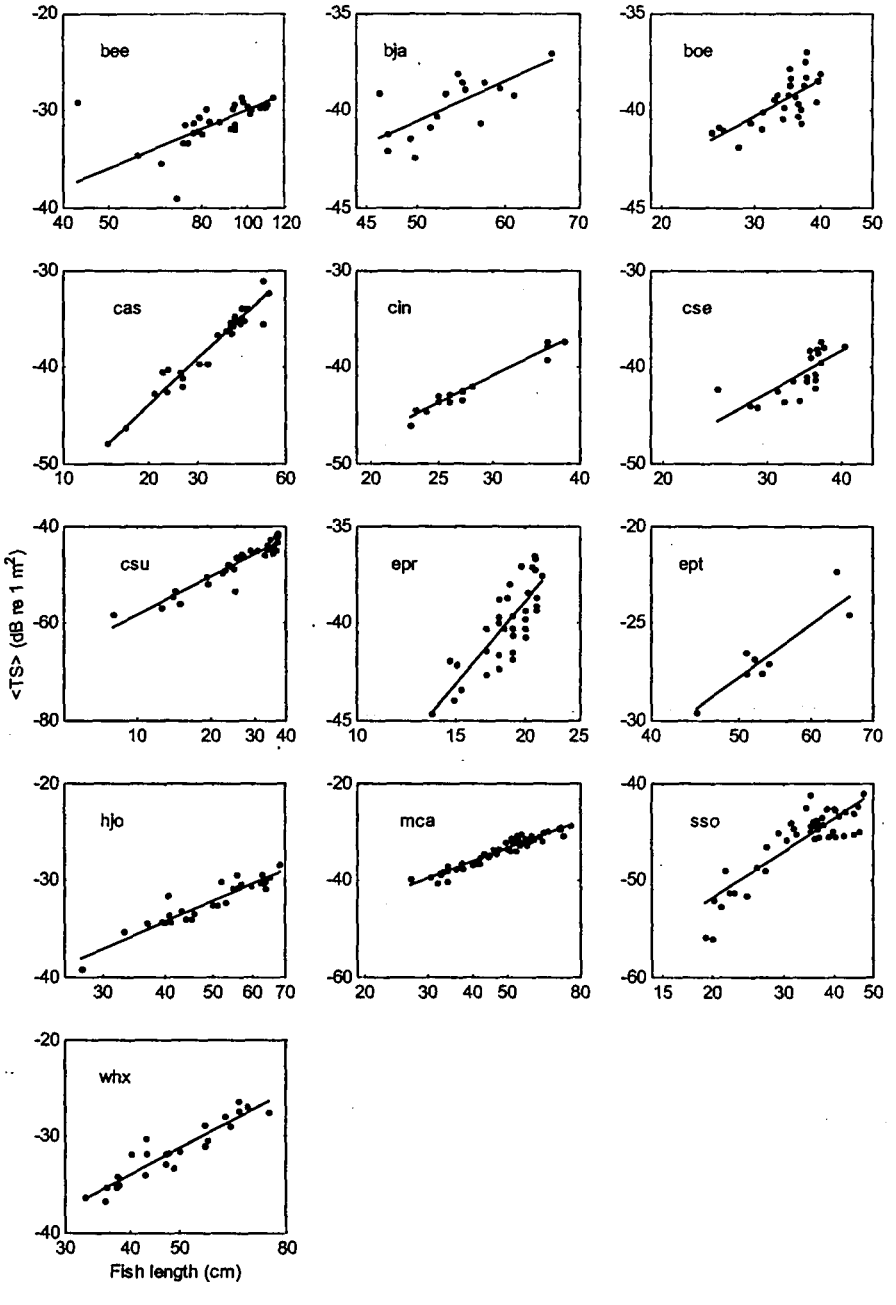

Figure 7: The swimbladder cast <TS> estimates and the regressions for each species in the analysis. The text on each sub-figure is the species code. Refer to Table 2 for species names. Only the 80% length, 1% weight points were used for the BOE regression.

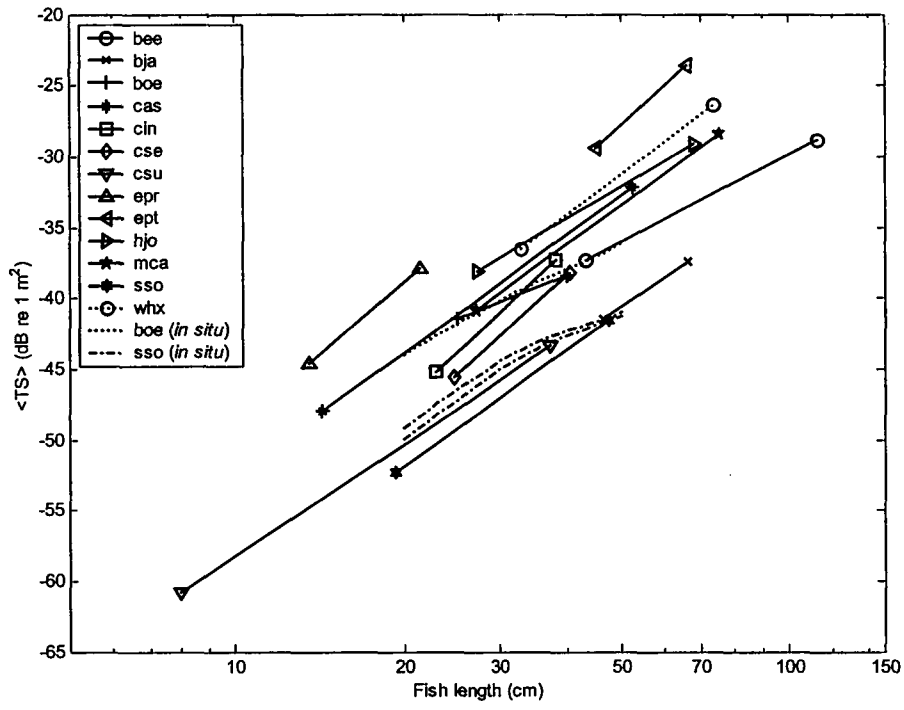

Figure 8: The fish length to <TS> relationships estimated from the swimbladder casts and Monte-Carlo *in situ* analysis. Only the 80% length, 1% weight points were used for the BOE regression.

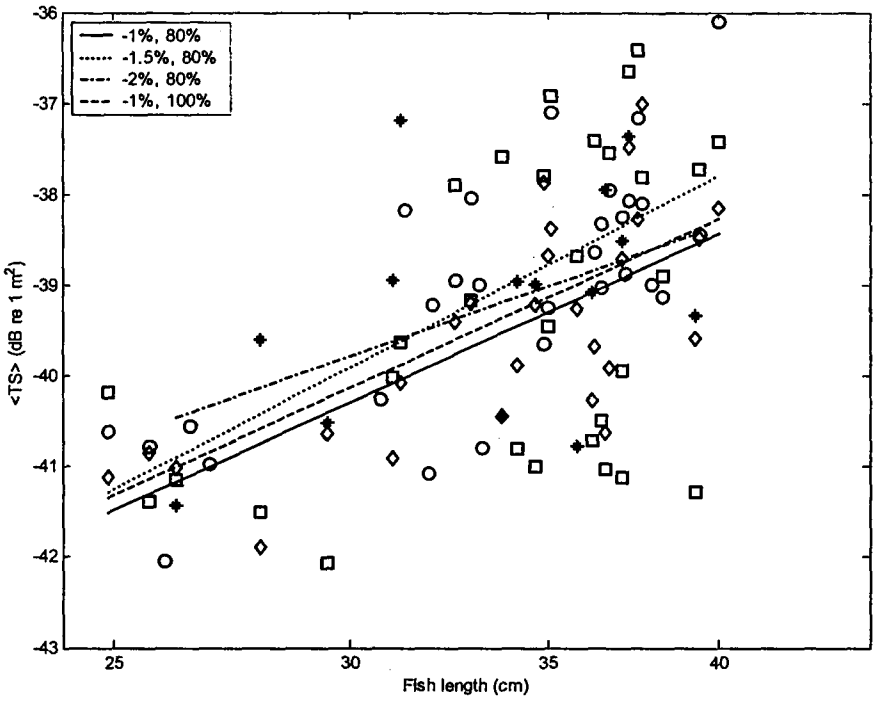

Figure 9: The swimbladder cast <TS> estimates for black oreo with varying cast volumes and cast lengths. The diamonds represent the –1%, 80% fish, circles the –1.5%, 80% fish, stars the –2%, 80% fish and squares the –1%, 100% fish.

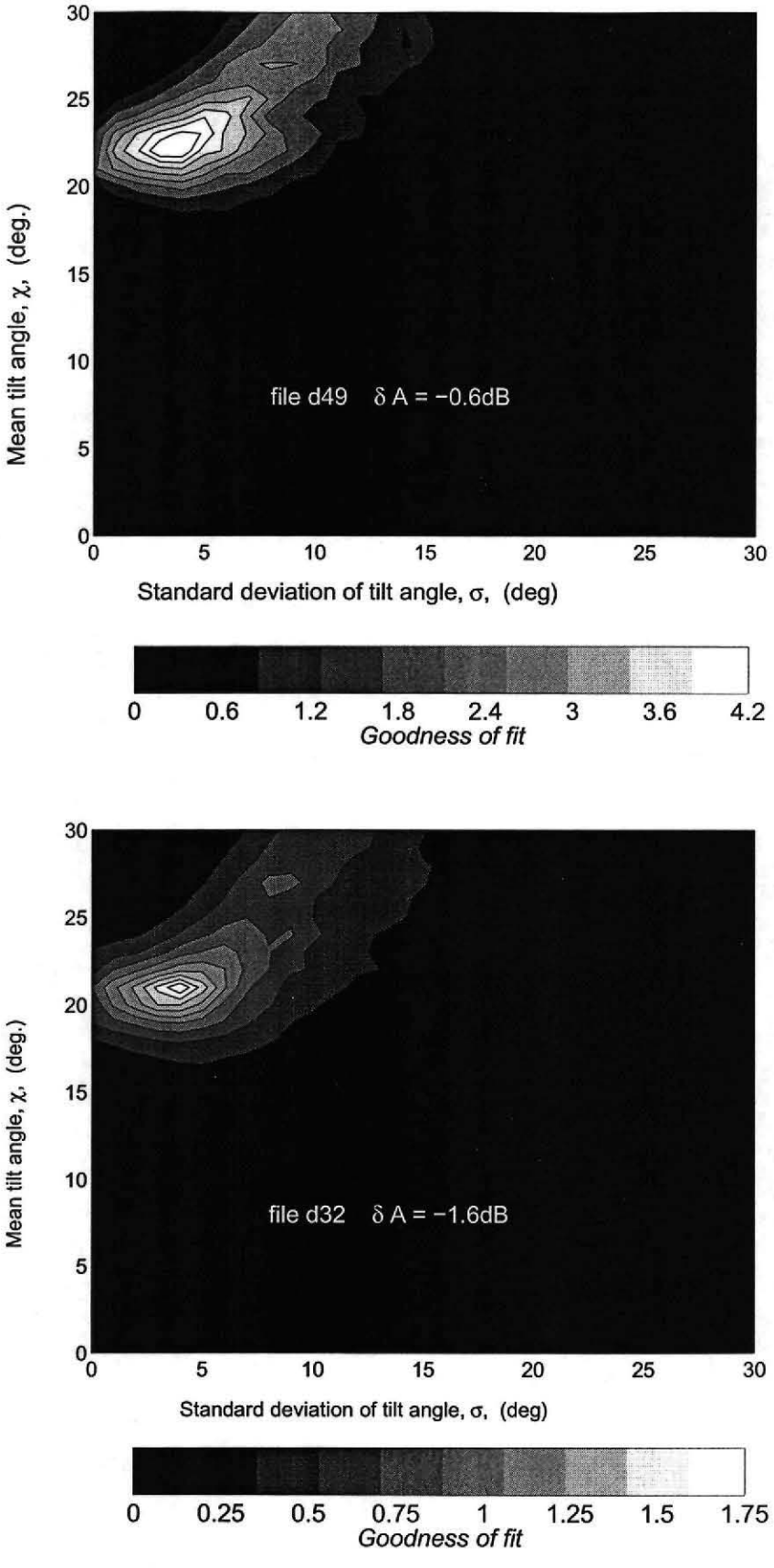

Figure 10: Goodness of fit contours plotted in tilt angle verses tilt angle standard deviation space. Lower panel: transect d32. Upper panel: transect d49.

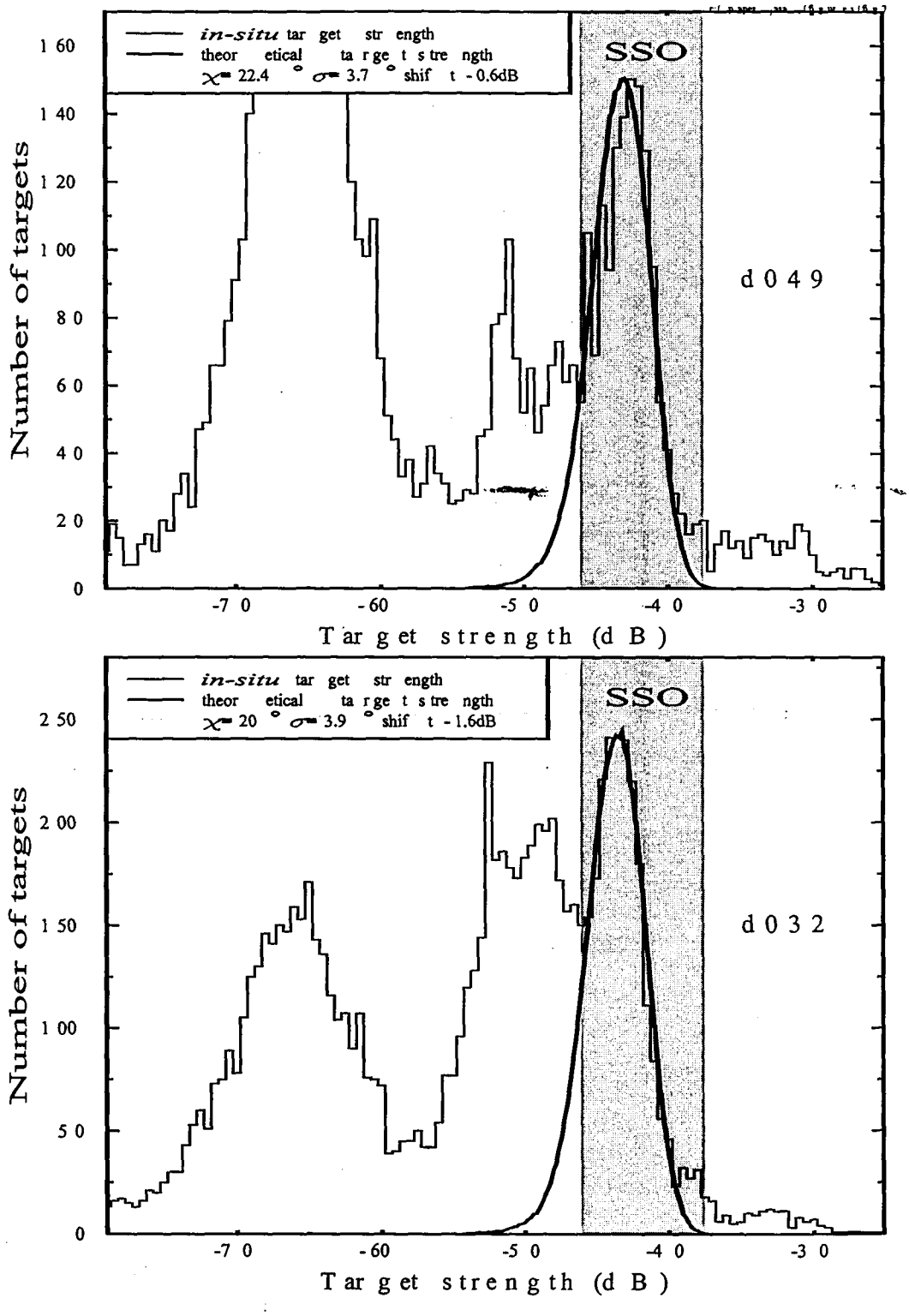

Figure 11: Comparison of target strength data derived from modelling with target strength data measured in-situ. Lower panel: transect d32. Upper panel: transect d49.

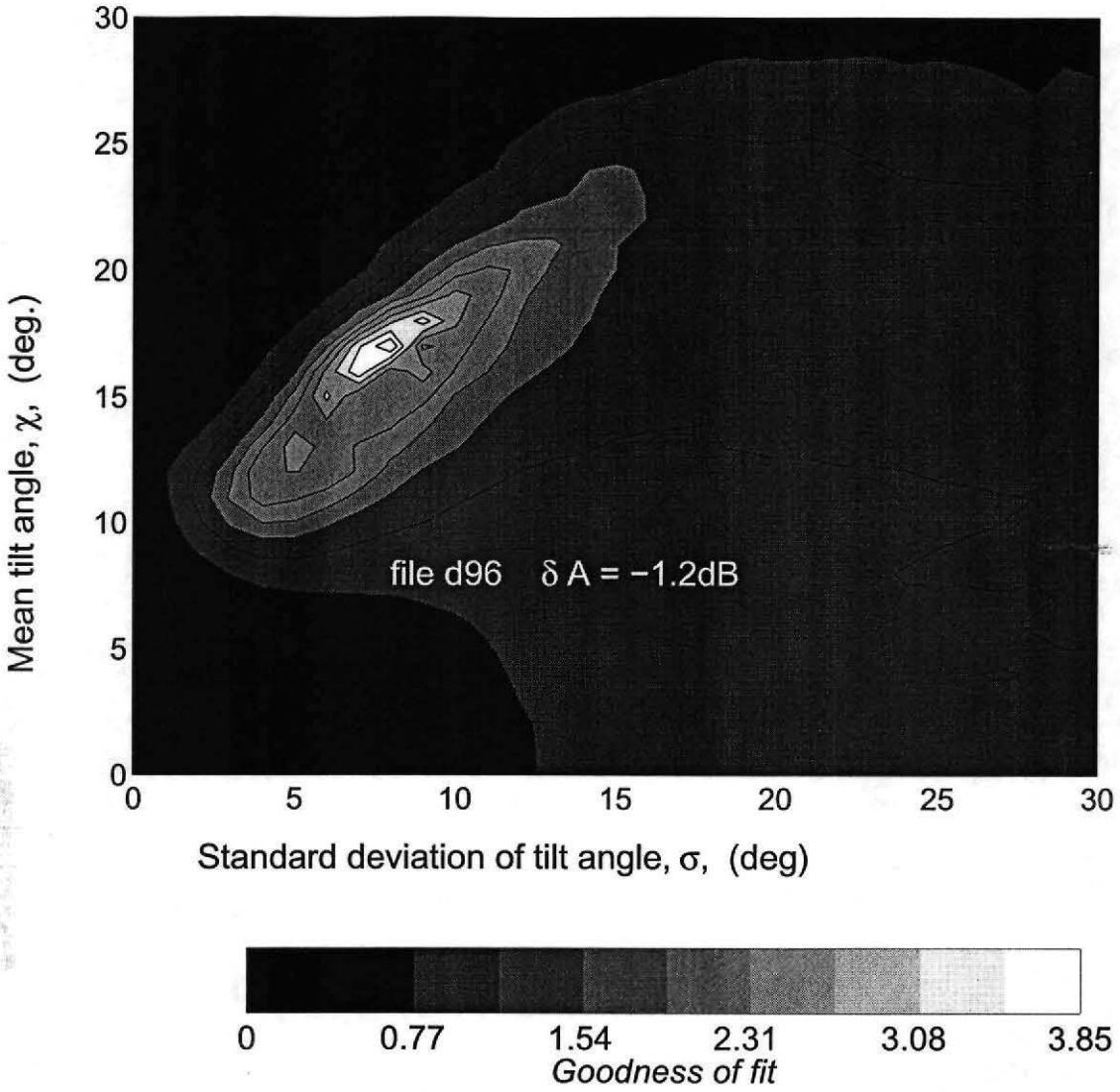

Figure 12: Goodness of fit contours plotted in tilt angle verses tilt angle standard deviation space. Transect d96.

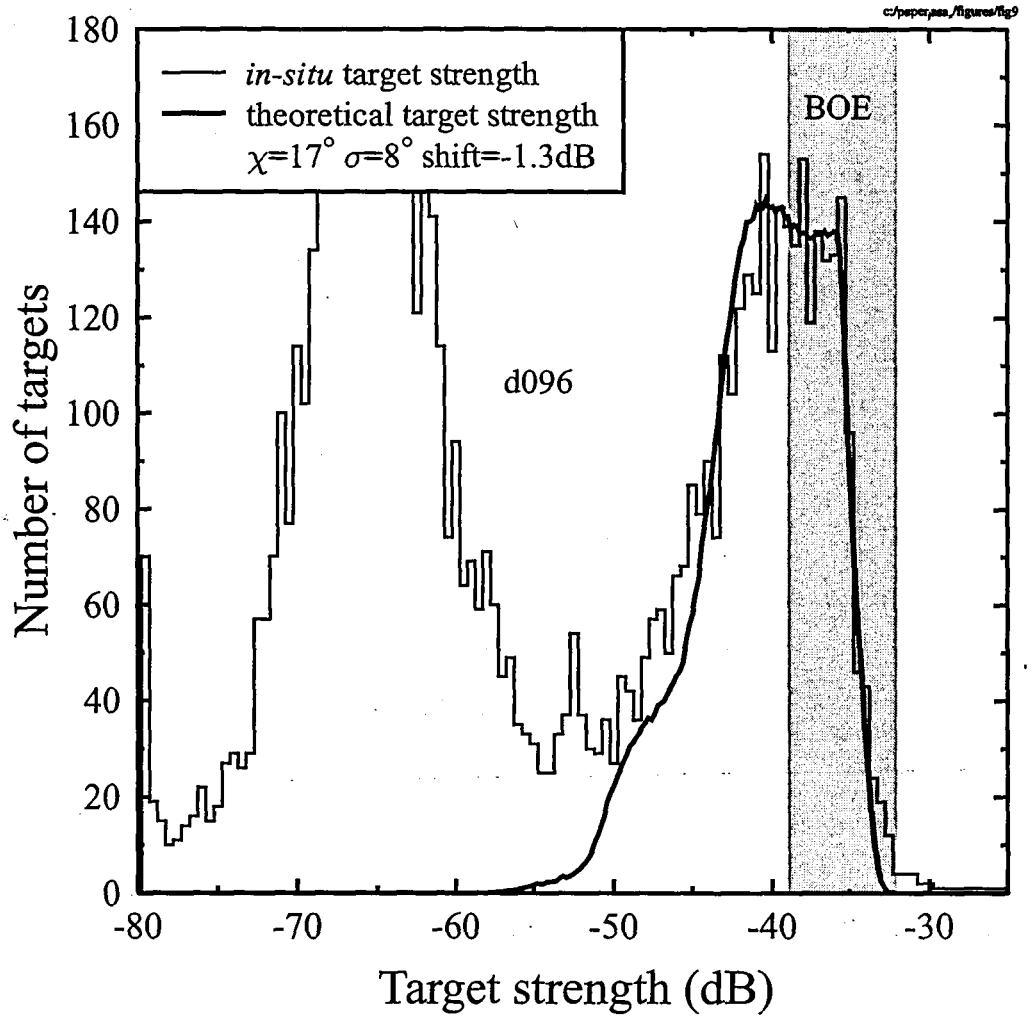

Figure 13: Comparison of target strength data derived from modelling with target strength data measured *in situ*. Transect d96.

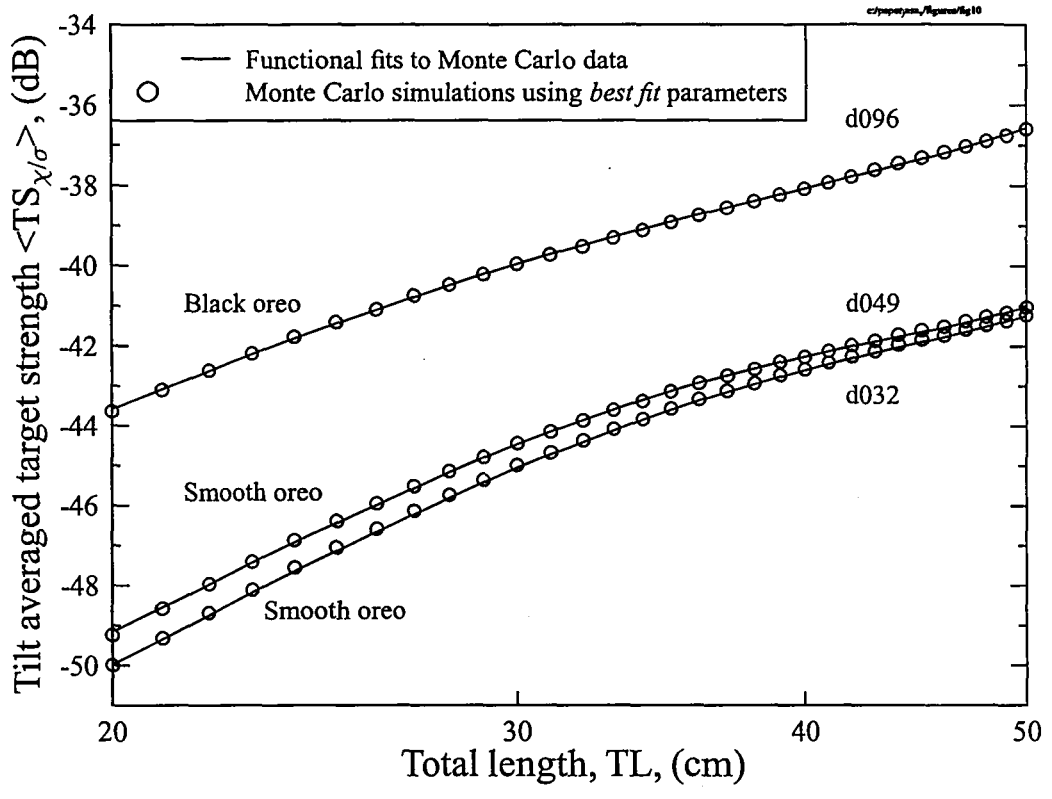

Figure 14: Tilt averaged target strength data plotted as a function of fish total length for black and smooth oreo.

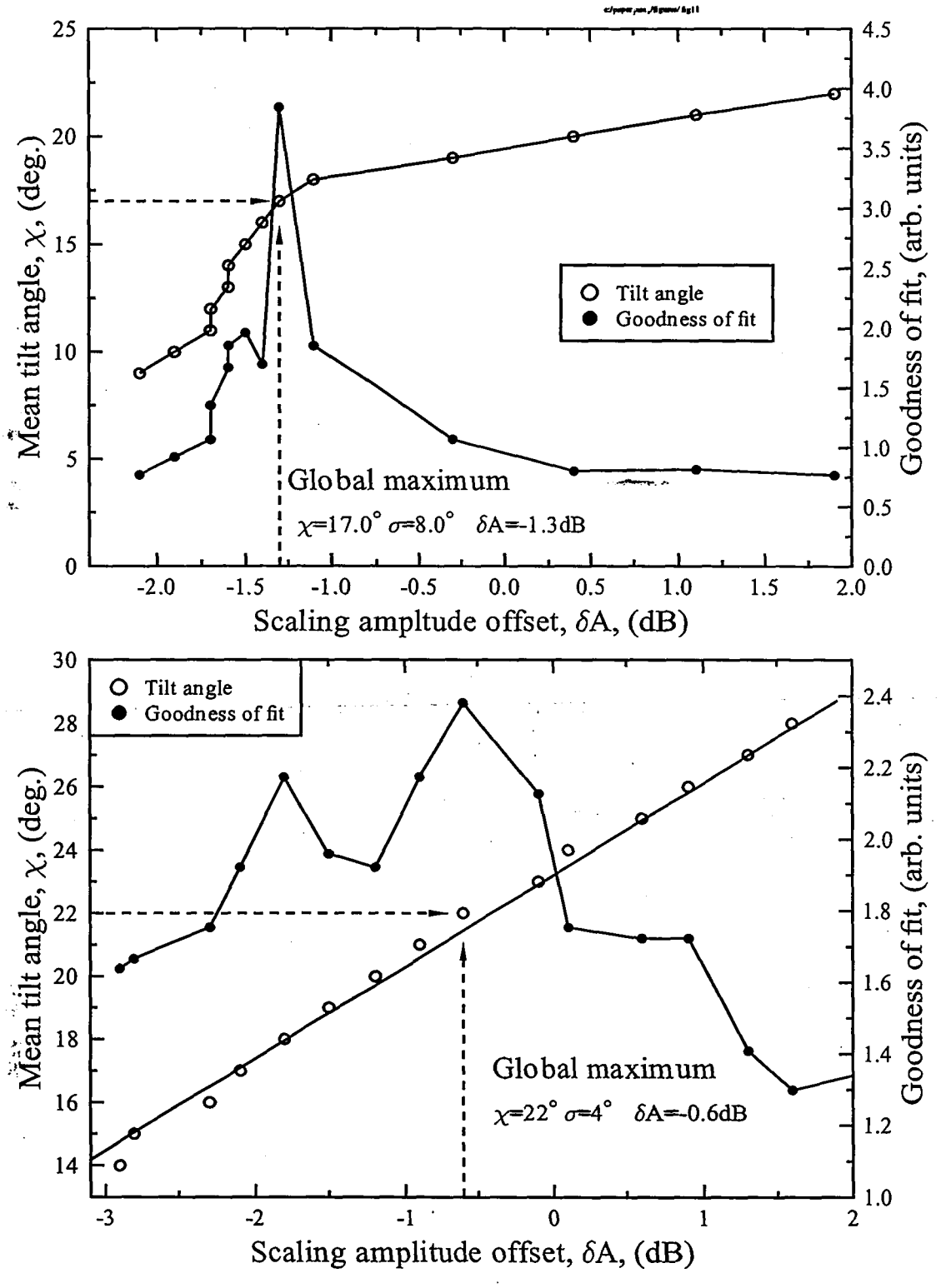

Figure 15: Mean tilt angle and goodness of fit plotted as a function of the scaling amplitude offset. Lower panel: transect d49. Upper panel transect d96.

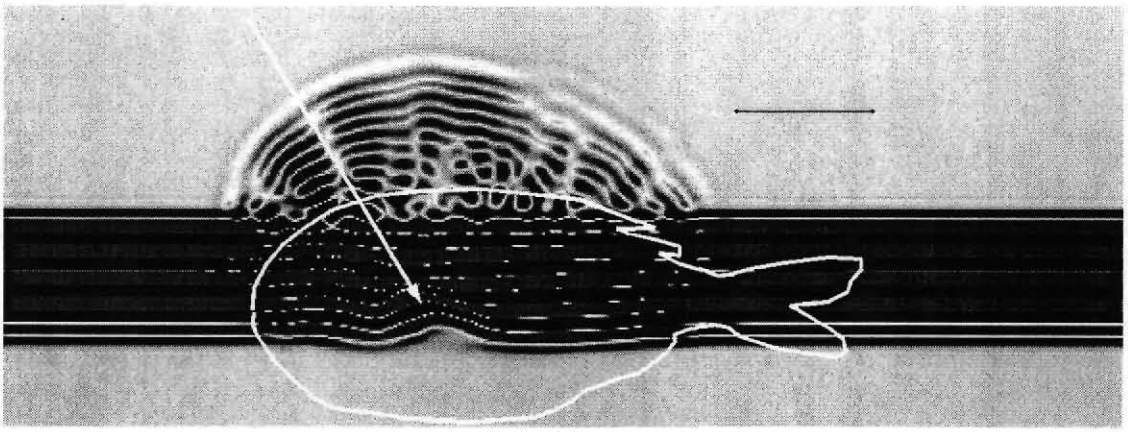

Figure 16: The wave field scattered by fish 1 at 16 μs into the simulation. The arrow indicates the retarding of the incident wave by the wax-ester in swimbladder, which has a slower sound speed than in the rest of the fish. The image is a slice midway through the z-axis of the 3D computation volume. The position of the fish is given by the white outline. The colours represent acoustic pressure, with blue corresponding to low pressure and red to high. The horizontal line is 100 mm long.

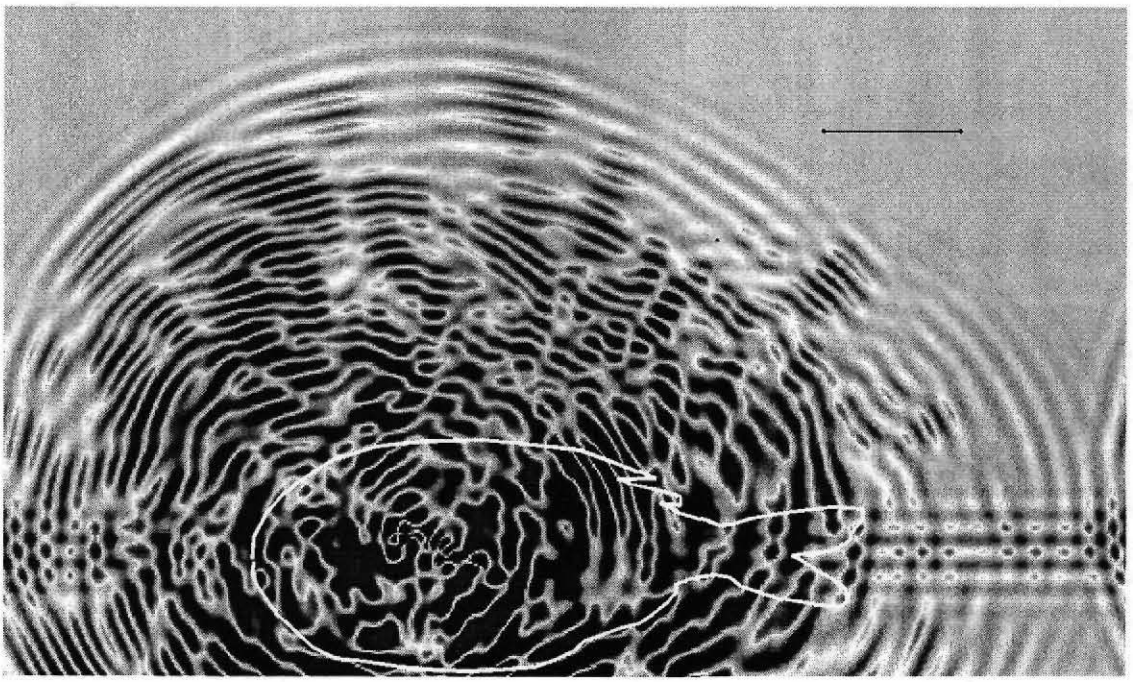

Figure 17: The wave field scattered by fish 1 at 34 μs into the simulation. The incident wave as passed completely through the fish and a faint reflection from the lower boundary can be seen. The image is a slice midway through the z-axis of the 3D computation volume. The position of the fish is given by the white outline. The colours represent acoustic pressure, with blue corresponding to low pressure and red to high. The horizontal line is 100 mm long.